Indian Journal of Engineering & Materials Sciences
Vol. 24, April 2017, pp. 147-152

Effect of minor Zr addition on γ′ and η phase precipitation and tensile properties of A286 superalloy

Masoumeh Seifollahi[a]*, Seyed Hossein Razavi[b], Shahram Kheirandish[b,c] & Seyed Mahdi Abbasi[a]

[a]Metallic Materials Research Center, Malek ashtar University of Technology, Tehran, Iran

[b]School of Metallurgy and Materials Engineering, Iran University of Science and Technology, Tehran, Iran

[c]Center of Excellence for High Strength Alloys Technology, Iran University of Science and Technology, Tehran, Iran

Received 16 February 2016: accepted 19 January 2017

In this study, the mechanisms of Zr on microstructure and tensile properties of A286 Fe-based superalloy were investigated. Cellular η phases precipitated homogenous at approximately all the grain boundaries in the modified Zr-A286 superalloy but heterogeneous in Zr-free alloy. Detailed microstructural analysis revealed that with the addition of Zr to the alloy; the grain size reduced, η volume fraction decreased and the growth and dissolution of γ′ phase accelerated. The mechanism of Zr in Ni and Fe-based superalloys is different. The mechanism in Fe-based superalloy is segregation of Zr at grain boundaries and occupation of Ti sites for η phase formation. In Ni based superalloy, Zr stabilizes the γ′ phase and retards the γ′ to η transformation. Zr addition led to improvement of room temperature tensile strength by replacement of the primary relatively smooth grain boundaries by new jagged grain boundaries after the η phase precipitation.

Keywords: Fe-based A286 superalloy, Zr addition, η phase, Tensile strength

Fe-based austenitic superalloys such as A286 are widely used in gas turbine industry at intermediate elevated temperature services[1]. These alloys strengthen by the spherical ordered γ' (fcc-$Ni_3(Al,Ti)$) precipitates. The γ' phase is unstable after aging treatment at high temperature, so dissolves and the stable η (hcp-Ni_3Ti) phase precipitates[2]. Depending on the chemical composition and heat treatment conditions, the γ' and η phases precipitate simultaneously or sequentially in this alloy system[3,4]. It is widely known that the precipitation of η phase is related to the decreased stress-rupture life. So, the η phase is considered as deleterious minor phase, because it usually poses negative impact on the mechanical properties of superalloys[5]. Thus, efforts to modify the chemical composition of A286 and similar Fe-based superalloys to retard the formation of η phase are indispensable. Many studies have been undertaken to improve the elevated temperature properties of γ' strengthened superalloys by chemical composition modification and proper heat treatment[6-9]. Zhao *et al*.[1] demonstrated that addition of boron traces in the modified A286 could inhibit the cellular η phase from precipitating at grain boundaries and significantly improved ductility and alleviated hydrogen damage of the alloy. Zhao *et al*.[3], and Cui *et al*.[6], determined that the structural stability of the Ni-Co-based superalloy, Inconel 740, can be improved by adjusting Al, Ti and Si levels in the alloy. These modified alloys exhibit a more stable structure during aging as γ' become more stable and the transformation of γ' to η retards. Long *et al*.[7] showed that a high Ti+Al content in a Ni-based superalloy, GTD-111, would favour the formation of the η phase in the interdendritic region. It is reported[10] that the γ′ phase is intensified and more stable after Zr instead of Al in Ni-based superalloys and consequently, the transformation of γ' to η would retards[6]. However, there is hardly any sufficient and efficient study investigating the effects of Zr addition on the precipitation mechanism of γ′ and η in Fe- based superalloys such as A286. Although extensive research has been focused on the effect of η on mechanical properties, less attention has been paid to the effect of the alloying elements, especially that of Zr, on it. Thus, the influence of Zr on the microstructure, η and γ' phases precipitation mechanism in A286 superalloy is assessed in the present study.

Experimental Procedure

The chemical compositions of the two alloys are given in Table 1. Master ingots were melted in a vacuum induction melting furnace (Balzers type,

*Corresponding author (E-mail: m_seifollahi@alumni.iust.ac.ir

Table 1 — Chemical compositions of experimental alloys (wt%)

Specimens	Fe	Ni	Cr	Mo	Mn	Si	C	B	Ti	Al	Zr
Zr-free A286	bal	25.8	13.6	1.07	0.90	0.10	0.003	0.001	2.32	0.23	0
Zr-A286	bal	25.7	13.4	0.99	0.95	2 0.1	0.003	0.001	2.42	0.24	0.05

Germany) and cast into cylindrical bars with a diameter of 45 mm and a length of 200 mm. The furnace was evacuated to 10^{-3} Pa and purged with high purity argon. All raw materials were rinsed separately with acetone and charged into a MgO-15%Al_2O_3 crucible, but aluminium, ferroboron, ferrozirconium and manganese were charged after full melting of the charged materials. The pouring temperature was 1300 ± 20°C. The ingots were solidified in equiaxed condition and cooled in evacuated chamber. Cast ingots were homogenised at 1180°C for 5 h and subsequently hot-rolled at 1150°C to a reduction of 80%[11,] The rolled products were solution annealed at 980°C for 1 h, followed by water quenching.[12,] 10 × 10 × 10 mm samples were exposed to accelerated aging tests in the temperature range of 650-900°C for 1-30 h to evaluate the η phase. The electrical resistance furnaces used in this research had an accuracy of about ±5 K.

Metallographic sections were prepared using standard mechanical polishing procedures and etched with a 15 mL HCl, 8 mL HNO_3 and 4 mL glycerin solution. A Vega Tescan SEM equipped with EDS analyser operating at 15 kV, and optical microscopy (OM) were used to observe the morphology and distribution of phases. Volume fraction of η phase and the grain size was calculated by Image Analyser Clemex software and systematic manual point count method.[13]

Thermodynamic calculations were performed to predict the phase stability in the alloy composition using the Thermo-Calc[14,] program and Ni database established by Thermo-Tech Co. No modification was made to the database, and the only input to the calculations was the alloy composition.

Tensile tests at room-temperature were carried out on an Instron Model-8502 test machine. Tensile tests were conducted in accordance with ASTM E8[15] of the tension testing of metallic material. Each datum was an average of at least three tensile tested values.

Results and Discussion

Microstructure evolution

Microstructure observation of the Zr-free A286 and Zr-A286 after aging heat treatment at 800, 820 and 840ºC is presented in Fig. 1. It can be seen that the microstructure consists of (I) austenitic grains, (II) annealing twins and (III) η phases. As shown, the microstructure changes with aging temperature and also Zr addition. Table 2 shows the grain size of both alloys at different ageing temperatures and times.

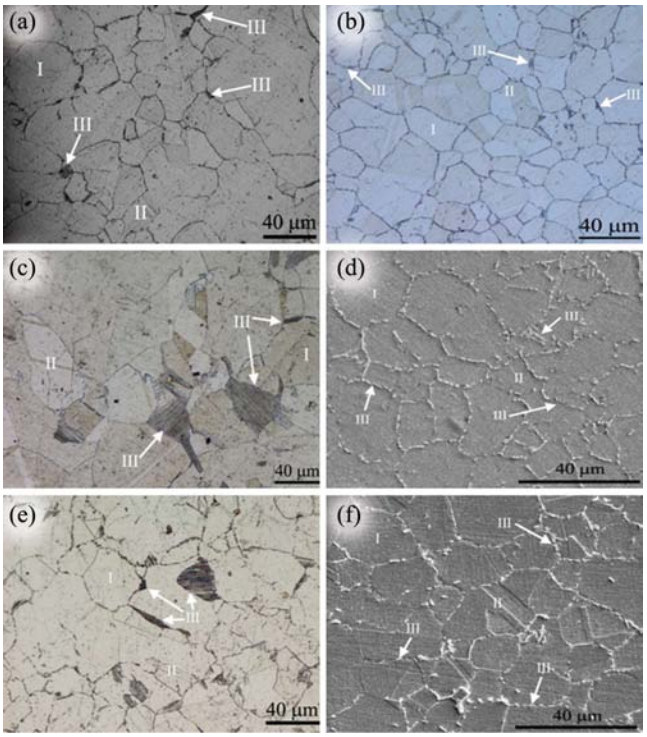

Fig. 1 — Optical microstructure of the Zr-free alloy aged at (a) 800°C for 16 h; (c) 820°C for 16 h and (e) 840°C for 4 h and Zr-A286 alloy aged at (b) 800°C for 16 h; (d) 820°C for 16 h and (f) 840°C for 4 h (I:austenitic grain; II: twinning; III: η phase)

Figure 2 presents the variation of η phase volume fraction with aging temperature for 4 h. The amount of η phase for the Zr-free alloy is listed for comparison as well. With an increase the aging temperature, the η volume fraction increases. Ti atoms diffuse to high energy areas and η phase will nucleate by increasing the aging times and temperatures.[2] Furthermore, with an increase the times and temperatures, coarsening and coagulation of the γ' phase occurs.[16] So, the coagulated γ' dissolves and the phase transition of γ'→ η occurs. The effect of aging time and temperature has been investigated by the authors and well illustrate in Ref. [11]

Composition also has an effect on the η phase volume fraction and morphology. Comparing the microstructures of Zr-free and Zr-A286 alloys (Fig. 1) confirms that with Zr addition: the grain sizes decrease from about 40 to 20 μm (Fig. 1 and Table 2); the

Table 2 — Grain size of the alloys

Specimen	Aging temperature, ºC	Aging time, h	Avg. grain size, μm
Zr-free A286	800	16	47
	820	16	60
	840	4	51
Zr-A286	800	16	25
	820	16	26
	840	4	18

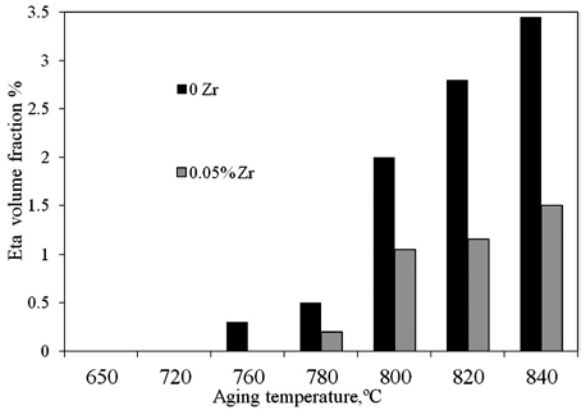

Fig. 2 — Variation of η volume fraction with aging temperature for 4 h

cellular η phase volume fraction decreases; and the Widmanstätten η phase does not form.

The role of Zr on the grain size is closely related to the fact that, Zr atoms segregate at the grain boundaries. The EDS results show that the amount of Zr is 0.054 and 0.034 into the grain and at the grain boundary respectively. The researchers[17-20], reported that the segregation of Zr at the grain boundaries was detectable in Ni-based and Fe-based superalloys. Zr is relatively a heavy element with slow diffusion rate. Hence, Zr segregation at the grain boundaries pin the boundaries and prevent the grain growth during annealing and subsequent overaging. So, the Zr-A286 has finer grain size than Zr-free alloy.

There are large amounts of cellular η phase, precipitated at the grain boundaries and interior the grains in the Zr-free alloy. This phase, with a nominal composition of Ni_3Ti, was also described by the authors in Ref.[11] As it is shown in Fig. 2, in Zr-free alloy, the η phase forms at 760ºC, but in the Zr-A286, the η formation temperature increases to 780ºC and its amount decreases at the same temperature. For instance, the η volume fraction in the Zr-free alloy aged at 840ºC for 4 h is 3.45% that declines to 1.5% by addition of 0.05 wt% Zr. The basis for Zr-retarded precipitation of η phase can be as follows: first, for the alloy quenched from high temperature, Zr preferred to take the sites at grain boundaries. Thus, there will be

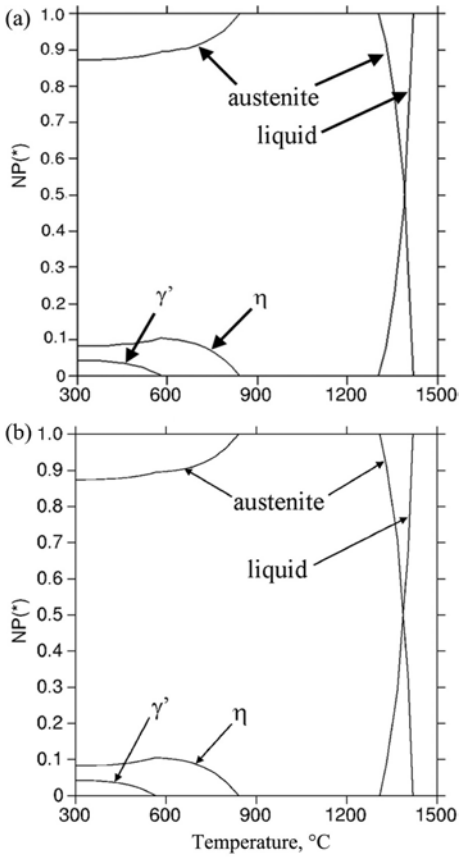

Fig. 3 — Calculated phase fraction as function of temperature for experimental alloy (a) 0.05 wt% Zr and (b) 0 wt%Zr

fewer sites for η nucleation. Second, it is believed that γ′ phase tend to decompose into η phase through grain boundary reaction, and its nucleation and growth process is controlled by grain boundary diffusion. The nucleation of η phase is controlled by the diffusion of Ti atoms at grain boundary. However, the growth of η phase is mainly closed related to the diffusion of Ti atoms within the grains.[1] Therefore, segregation of Zr at the grain boundaries would cause a decrease of the boundary diffusivity of Ti atoms along the grain boundaries, and efficiently retard the nucleation and growth of η phase in the alloy.

Thermodynamic calculation was performed to predict the phase stability in the alloy. The result, using the representative composition in Table 1, is shown in Fig. 3a and b. Figure 3a shows all the predicted equilibrium phases of Zr-alloy and their weight fractions at each temperature. For instance, at 1450ºC (above the liquidus), only the liquid phase forms. The γ phase and liquid phase coexist at temperatures between 1305°C and 1420ºC, and their weight fractions change with temperature. The η and γ′ phases exist at low temperature and dissolve into the matrix at

840°C and 579ºC, respectively. The equilibrium phases calculate in Fig. 3b for Zr-free alloy and the results compares with Zr-alloy in Table 3. The calculated data shows that the γ′ solves temperature ascends with addition of Zr, the amount of η phase decreases and the others data remains unchanged. These results of thermodynamic predicted data based on Ni database will compare to the experimental data to find the mechanism of Zr on η phase in Fe-based and Ni-based superalloy.

In the following, the effects of Zr addition on γ′ phase in Fe-based A286 superalloy are also studied. High-resolution SEM was employed to study the effect of Zr on the γ′ size for the alloys after aging heat treatment. The microstructures of the alloys which consist of γ, γ′ and η phases are shown in Fig. 4. The spherical morphology of γ′ phase is visible. This figure reveals the variations of γ′ phase size in Zr-free and Zr-added alloy at different aging temperatures and times. For instance, the γ′ particle size of samples aged at 840ºC was measured and exhibit in Table 4.

However, it is reported[10] that in Ni-based superalloys; Zr atom loses outer electrons, which is of benefit for the Zr atom to dissolve in the γ′ phase. It indicates that the γ′ phase is intensified and is more stable after Zr instead of Al in the system. When the γ′ get stable, the γ′ to η transformation retards and the η volume fraction increases. In addition, the thermodynamic calculation based on Ni-database in Table 3 proves these statements.

According to Fig. 4, the γ′ phase sizes and the distance between γ′ particles in the Zr-free alloy is less than those of Zr-alloy. It shows that Zr accelerate the growth and solution of γ′ and destabilize γ′. It is in contrast to the effect of Zr in Ni-based superalloy.[10] So, the mechanism of Zr on η phase in Fe-based alloy is different to Ni-based alloy. For both alloys, the formation of η phase has been suppressed by Zr addition, but by different mechanisms. The mechanism of Zr in Fe-based superalloy is segregation of Zr at grain boundaries and occupation of Ti sites for η phase formation. In Ni-based superalloy, Zr stabilizes the γ′ phase and retards the γ′ to η transformation.

Table 4 — The γ′ particle size of Zr-free and Zr-A286 after aging

Specimen	Aging temperature, ºC	Aging time, h	Avg. dia. γ′ particle, μm
Zr-free A286	840	4	72
Zr-A286	840	4	158
Zr-free A286	840	8	92
Zr-A286	840	8	348
Zr-free A286	840	16	145
Zr-A286	840	16	55

Tensile properties

Room temperature tensile tests were performed on the solution treated alloys aged at 820°C for 16 h and air quenched. In this condition, both alloys contain η phase. According to Figs 1 and 2, Zr-free alloys have more fraction of η phase than Zr-alloy. The experimental stress versus strain curves are presented in Fig. 5. The variations of ultimate tensile strength (UTS) and elongation (El-%) of the alloys as a function of Zr content are illustrated in Fig. 6. As Fig. 6 depicts, with Zr addition, UTS increases from 719 MPa to 747 MPa and El-% increases from 36% to 39%. The results show that Zr can significantly improve both room temperature tensile strength and ductility. Usually, if strength increases the ductility comes down, but in this case with the addition of Zr, the grain size decreased so the ductility and strength increase simultaneously.

According to the precipitation mechanism for η phase outlined by Xu *et al*.[21], the precipitation of the η phase induces the orientation of cellular austenite to transform to the same as that of the neighboring grain. It is worth to note that the η phase shows a cellular morphology, that is, lamellar η phase in cellular austenite colonies. Therefore, the primary relatively smooth grain boundaries will be replaced by new jagged grain boundaries after the η phase precipitation. The jagged grain boundaries can restrain grain boundary sliding and prevent it from cracking during deformation. Although, according to Fig. 1, the Zr-alloy has fewer amount of η phase than Zr-free alloy, but all the grain boundaries of Zr-alloy decorates by η phases with smaller size than in Zr-free alloy. Additionally, in Zr-free alloy, η phases precipitated in some of the grain boundaries not all of them. As a result, Zr-alloy has more fractions of jagged grain boundaries and more tensile strength. Furthermore, Zr-added alloy has finer grains than Zr-free alloy. The room temperature tensile results correlate to grain size according to the long established Hall-Petch

Table 3 — calculated data for eta and γ' phases

Specimen	Max η volume fraction, vol%	Max γ' volume fraction, vol%	η solution temperature, °C	γ'Solution temperature, °C	Temperature of max η, °C
Zr-free A286	1.04	0.0417	840	563	580
Zr-A286	1.02	0.0417	840	579	583

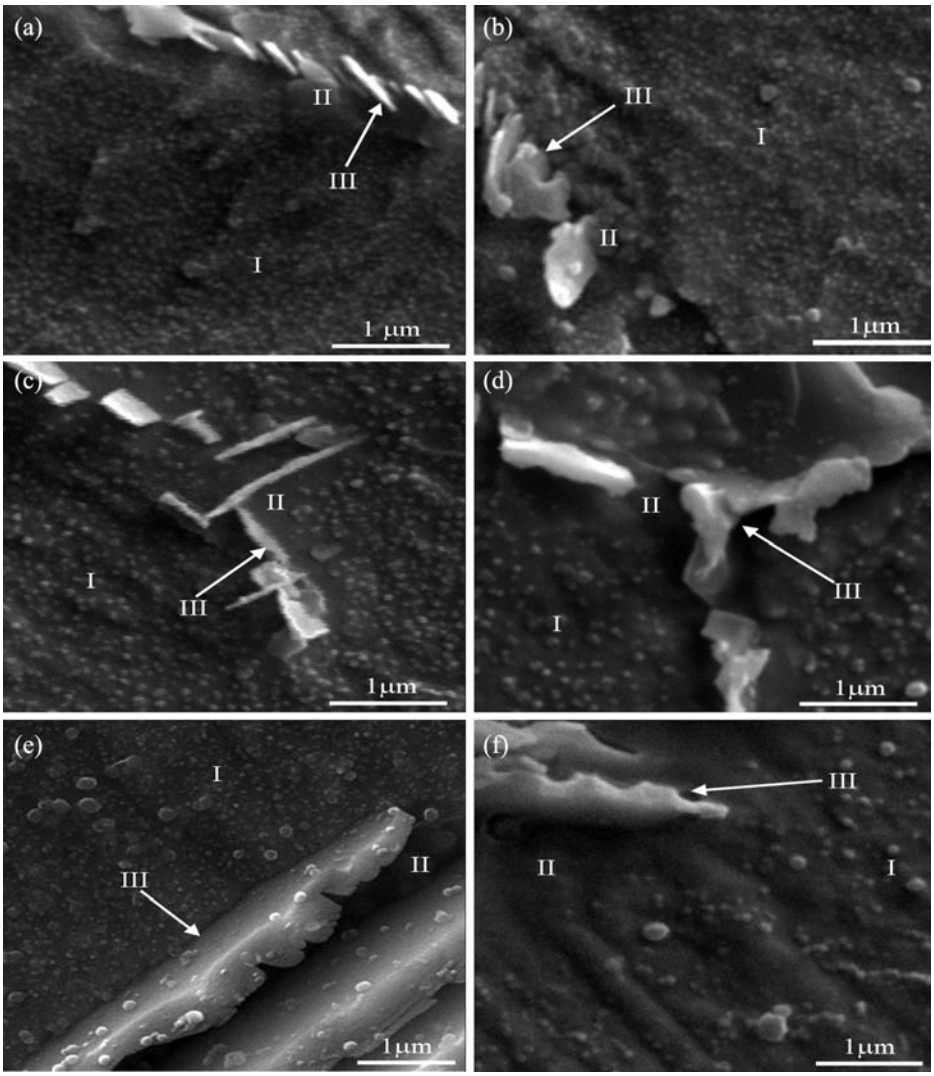

Fig. 4 — SEM microstructure of the Zr-free alloy aged at (a) 780°C for 16 h; (c) 820°C for 16 h and (e) 840°C for 8 h and Zr-A286 alloy aged at (b)780°C for 16 h; (d) 820°C for 16 h and (f) 840°C for 8 h (I: γ′in austenitic matrix; II: γ′ free zone; III: η phase)

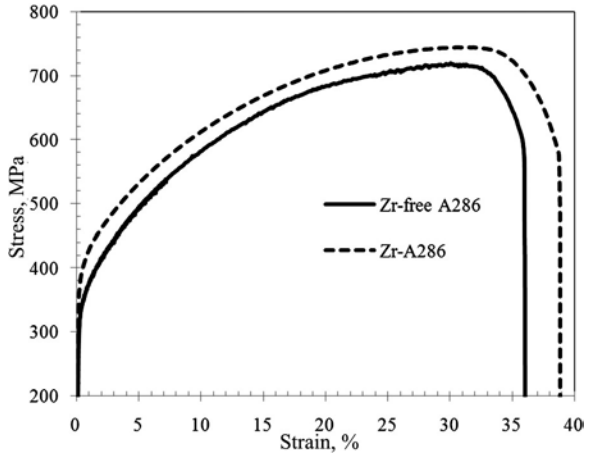

Fig. 5 — Strain–stress curves of alloys aged at 820ºC for 16 h after tensile test at room temperature

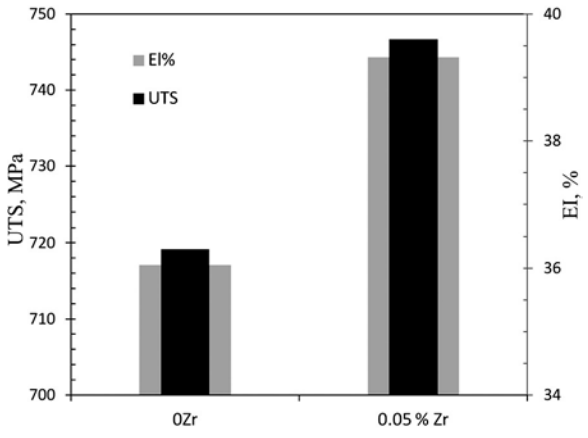

Fig. 6 — UTS and Elongation for specimens aged at 820ºC for 16 h after tensile test at room temperature

relationship. Hence, fine grained Zr-added alloy is best for improving strength.

Conclusions

Based on the findings of the present study, the following conclusions are drawn:

(i) Detailed microstructural analysis revealed that with the addition of Zr to Fe-based superalloy; the grain size reduced about 20 μm, the volume fraction of η phase decreased and the growth and dissolution of γ′ phases accelerated.

(ii) All the grain boundaries of Zr-A286 decorated by η phases with smaller size than in Zr-free alloy.

(iii) It is found that, the mechanism of Zr on η phase in Fe-based alloy is different from Ni-based alloy.

(iv) Zr addition led to improvement of room temperature tensile strength. The primary relatively smooth grain boundaries will be replaced by new jagged grain boundaries after the η phase precipitation and prevent cracking during deformation.

References

1 Guo Z, Liang H, Zhao M & Rong L, *Mater Sci Eng*, 527A (2010) 6620-6625.

2 Zhao M J, Guo Z F, Liang H & Rong L J, *Mater Sci Eng*, 527A (2010) 5844-5851.

3 Zhao S, Xie X, Smith G D & Patel S J, *Mater Des*, 27 (2006) 1120-1127.

4 Rho B S & Nam S W, *Mater Sci Eng*, 291A (2000) 54-59.

5 Xu Y, Zhang L, Li J, Xiao X, Cao X, Jia G & Shen Z, *Mater Sci Eng*, 544A (2012) 48– 53.

6 Cui C Y, Gu Y F, Ping D H, Harada H & Fukuda T, *Mater Sci Eng*, 485A (2008) 651-656.

7 Long F, Yoo Y S, Jo C Y, Seo S M, Song, Jin T & Hu Z Q, *Mater Sci Eng*, 527A (2009) 361-369.

8 Wen-juan W, Guang-wei H & Bo D, *J Iron Steel Res Int*, 17 (2010) 64-69.

9 Kusabiraki K, Takasawa Y & Ooka T, *ISIJ Int*, 35 (1995) 542-547.

10 Zheng Y, Wang C, Gao Z, & Li K, *Solid State Commun*, 73 (1990) 643-649.

11 Seifollahi M, Kheirandish Sh, Razavi & S H, Abbasi S M, *Int J Mater Res*, 104 (2013) 344-350.

12 *Steel, corrosion and heat-resistant, bars, wire, forgings, tubing, and rings ,15Cr-25.5Ni-1.2Mo-2.1Ti-0.006B-0.30V, Consumable electrode melted, 1650°F(899°C) solution and precipitation heat treated*, 5737C, (AMS) 2001.

13 *Standard test method for determining volume fraction by systematic manual point count*, E562, (ASTM) 1999.

14 SSUB3: Ni-v5 database, Provided by Thermo-Calc Software v3, 2002/2004.

15 *Standard Test Methods for Tension Testing of Metallic Materials*, E8, (ASTM), 2000.

16 Seifollahi M, Kheirandish Sh, Razavi S H, Abbasi S M & Sahrapour P, *ISIJ Int*, 53 (2012) 311-316.

17 Xie S, Wang T, Lu J, Yang H & G. Zhao, *J Mater Sci Tech*, 15 (1999) 415-418.

18 Xu F & Guo, *Iron Steel Res Int*, 24 (1989) 48-53.

19 Chen Q Z, *Mater Sci Eng*, 385A (2004) 402-418.

20 Kindrachuk V, Wanderka N, Banhart J, Mukherji D, Genovese D D & Sler J R, *Acta Mater*, 56 (2008) 1609-1618.

21 Liu X, Jian Z, Lijian R & Yiyi L, *Mater Sci Eng*, 488A (2008) 547-553.